Available online at www.sciencedirect.com
ScienceDirect
Catalysis Today 132 (2008) 81–87
CATALYSIS TODAY
www.elsevier.com/locate/cattod

Liquid-phase reductive deposition as a novel nanoparticle synthesis method and its application to supported noble metal catalyst preparation

Yoji Sunagawa, Katsutoshi Yamamoto, Hideyuki Takahashi, Atsushi Muramatsu *

Institute of Multidisciplinary Research for Advanced Materials, Tohoku University, Katahira 2-1-1, Aoba-ku, Sendai 980-8577, Japan

Available online 16 January 2008

Abstract

In the present study, the liquid-phase reductive deposition as a novel nanoparticle synthesis method has been investigated and its application to supported noble metal catalyst preparation was also focused. As a result, the maximum loading of Pt was around 20 wt% with keeping the particle size below 2 nm, by the present technique based on the liquid-phase reduction method. The selective reductive deposition is characteristically performed by the adsorption of metal ion or complexes on the surfaces and hereby the reduction. Namely, the initial adsorption of metal ions or complexes is the key point of this technique. Hence, key points of this method are: (1) precise control of the metal complex by adjusting solute conditions, such as composition and structure of metal complex, (2) storing of the suspension until the equilibrium composition and (3) aging suspension at controlled temperature. The most important is the first one, as the adsorption of specific metal complex results in the generation of precursor solid on the surfaces of the supporting materials. By this novel method, not only Pt but also Au nanoparticles supported on various carriers were successfully obtained.

Keywords: Liquid-phase reduction method; ZrO_2; α-Fe_2O_3; Noble metal; Nanoparticles; Catalyst preparation

1. Introduction

The attempt to develop new preparation method of highly active supported catalysts has been tried by so many catalysis researchers, because every conventional method is not satisfactory for both demands of high loading and high dispersion of nanoparticles on a carrier material. Needless to say, metal loading reaches maximum for supported catalysts, so far as the total surface area is limited and particle size of the metal is not changed. The apparent maximum metal content is found considerably low, e.g., 2–5 wt% Pt in well dispersed Pt/Al_2O_3 catalysts prepared by the ion-exchange method [1], though the maximum Pt content is calculated as 36 wt% to a support, assuming that the diameter of hemispherical Pt metal is 1 nm and the specific surface area of the support is 200 $m^2\,g^{-1}$. Unfortunately, conventional preparation methods have substantial defects on stabilization of metal precursor species on supports so that nanometer level in particle size cannot be kept after the thermal treatment. Namely, for impregnation technique, high dispersion cannot be expected in principle, as precursor salts are physically covered on support material mainly due to the van der Waals interaction. High metal loading cannot be expected for ion-exchange method, since an equilibrium adsorption amount of precursor species is basically regulated by the surface area and then so many adsorbents are aggregated to form a particle as a solid. As a result, these conventional methods are lack of a concept of the particle growth on a specific surface as a result of a heterogeneous nucleation. Namely, an adsorption site of precursor on the surface is utilized as a nucleation center and then monomers necessary to the particle growth are supplied from outside, not from adsorbents. Hence, the nucleus number may be equal to that of an adsorption site. Consequently, the following respects are the most important: (1) the increase in adsorption amount of the metal precursor precisely controlled in its form and conditions and (2) the protection of growing particles from their tremendous aggregation.

On the other hand, we can presume that the preparation method of highly dispersed particles on a support is classified in the field of nanoparticle synthesis. Among various methods to prepare the nanometer-sized particles, the liquid-phase reduction method [2] is one of the easiest procedures, since nanoparticles can be directly obtained from various precursor compounds

* Corresponding author.
E-mail address: mura@tagen.tohoku.ac.jp (A. Muramatsu).

0920-5861/$ – see front matter © 2008 Elsevier B.V. All rights reserved.
doi:10.1016/j.cattod.2007.12.008

soluble in a specific solvent. It has been reported that Ni and Ni–Zn nanoparticles with a diameter from 5 to 10 nm and an amorphous-like structure were synthesized by the liquid-phase reduction method and that Zn addition to Ni nanoparticles promote the catalytic activity for 1-octene hydrogenation [3].

In this paper, we will focus on the concept of this method and will extend it to the preparation of noble metal supported catalysts, which will be used as an industrial process.

2. Experimental

2.1. Basic concept

Titania, alumina, zirconia, silica, active carbon, zeolite and silica–alumina are often used as supporting materials. The ion-exchange method is the technique of exchanging metal cation for the proton on the surface of a supporting material and the impregnation method is to prepare the supported catalyst by impregnating a support in metal salt solution and then drying, followed by calcining it. For both the methods, as-prepared catalysts are reduced by H_2 or CO before use in necessity. pH of the starting metal salt solution is remarkably effective to the catalytic performance, because a size of catalyst metal particle is changed by pH due to the dependency of the adsorptivity of the support on pH [4]. However, by the conventional catalyst preparation method, a metal loading (the amount of metal put on the support) could not be increased, while the size of metal particles is kept in several nm. For example, in the preparation of Pt catalyst supported on alumina, the Pt loading cannot exceed 3–5 wt% in order to reduce the size to be about 1–2 nm [1]. The attempt to increase the metal loading much more was failed owing to the agglomeration of the metal particles [1] and/or the poor selectivity in their deposition onto the supports [5]. On the other hand, the catalytic activity of noble metals strongly dependent on the particle size [6] is maintained by inhibiting aggregation and sintering [7]. In addition to the increase in the specific surface area, a significant increase in surface density of unsaturated kink sites is expected of nanoparticles, leading to the remarkable promotion of the catalytic activity [8] and/or selectivity [9].

In the present study, the maximum loading will be around 20 wt% with keeping the particle size below 2 nm. Selective reductive deposition is based on the liquid-phase reduction method. First, precursor metal salts were dissolved in aqueous or organic media. If it is completely homogeneous solution, nanoparticles are formed through homogeneous nucleation and the growth via precipitation. However, in the presence of the supports, nanoparticles are nucleated and grown on the surfaces of carrier materials. Generally speaking, homogeneous nucleation needs the supersaturation level higher than heterogeneous one. In the system consisting of support solid and metal salt solution, the nucleation occurs on the surfaces of the solid. The selective reductive deposition is performed by the adsorption of metal ion or complexes on the surfaces and hereby the reduction. Namely, the initial adsorption of metal ions or complexes is the key point of this technique. Hence, key points of this method are:

(1) precise control of the metal complex by adjusting solute conditions, such as composition and structure of metal complex,
(2) storing of the suspension until the equilibrium composition and,
(3) aging suspension at controlled temperature.

The most important is the first one, as the adsorption of specific metal complex results in the generation of precursor solid on the surfaces of the supporting materials.

2.2. Au catalysts

Established procedure will be described below. Namely, 5 cm^3 of 1.0×10^{-2} mol dm^{-3} $HAuCl_4$ was mixed with 10 cm^3 of 2.0×10^{-2} mol dm^{-3} NaOH at room temperature with stirring and distilled water was added to the mixture to make the total volume 25 cm^3. This solution containing 2.0×10^{-3} mol dm^{-3} $HAuCl_4$ and 8.0×10^{-3} mol dm^{-3} NaOH ($[OH^-]_0/[Au^{3+}]_0 = 4.0$) was aged quiescently for 24 h at room temperature to complete the hydroxylation of Au^{3+} ions. The color of the solution changed from yellow to transparent, while pH shifted from 10.81 to 6.02, by this aging. Then, 40 mg of a support powder was added to the solution and, after ultrasonic dispersion for 30 min, the suspension was aged in a laboratory oven preheated at 100 °C for 48 h. The pH was slightly changed by addition of support powder (e.g., from 6.02 to 5.90 with addition of 40 mg of α-Fe_2O_3) and finally became ca. 5.5 (e.g., 5.42 with addition of 40 mg of α-Fe_2O_3) after the aging at 100 °C for 48 h. Aging operation was done in the darkness.

2.3. The other noble metal catalyst

This novel technique will be extended to the selective deposition of noble metal nanoparticles of the platinum group (Ru, Rh, Pd, Ir and Pt) onto well-defined metal oxide particles, since these noble metals are widely used as active catalysts for numerous purposes. The established standard procedure will be described as follows. 5 cm^3 of 1.0×10^{-2} mol dm^{-3} noble metal salt ($RuCl_3$, $RhCl_3$, $PdCl_2$, H_2IrCl_6, or H_2PtCl_6) was mixed with 10 cm^3 of given concentration of NaOH at room temperature with stirring and distilled water was added to the mixture to make the total volume 25 cm^3. This solution containing 2.0×10^{-3} mol dm^{-3} noble metal salt was aged quiescently for 24 h at room temperature to stabilize the metal complexes. After 24 h, pH was stabilized to be ca. 7.0. Then, 40 mg of a support powder was added to the solution and, after ultrasonic dispersion for 30 min, the suspension was aged in a laboratory oven preheated at 100 °C for 48 h.

2.4. Purification and characterization

Since the suspension of the composite material obtained after aging contained soluble impurities, such as chlorides, the purification was carried out the following manner. First, it was washed repeatedly for three times through the combination of

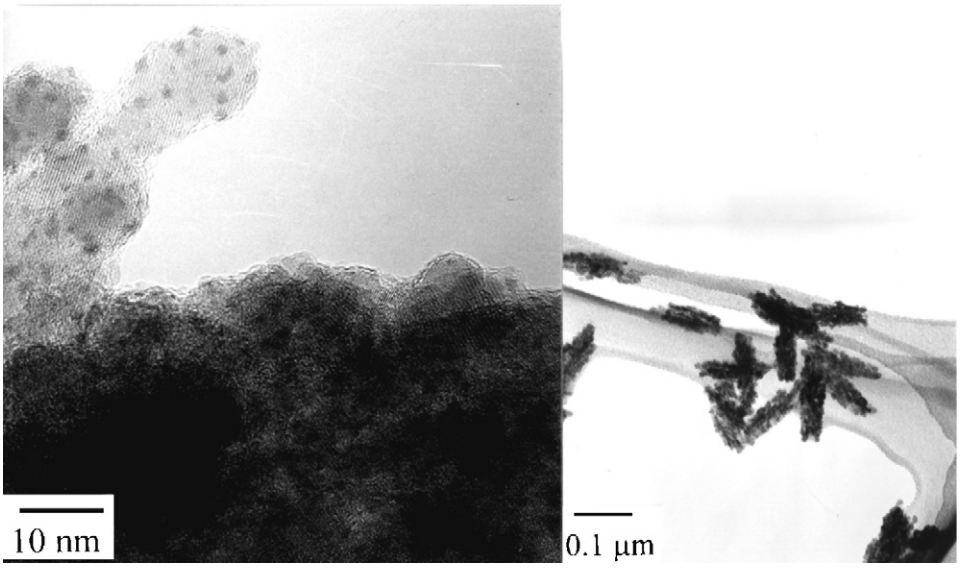

Fig. 1. Transmission electron micrographs of Au nanoparticles deposited on the surfaces of the polycrystalline ellipsoidal hematite particles. The left photograph is a close-up view of the right one.

centrifugal separation and ultrasonic dispersion in distilled water. Resultant solids were dried in air at 110 °C without further treatment such as calcination and reduction.

The purified solids were characterized by high-resolution transmission electron microscopy (HR-TEM, JEOL Co. Ltd. JEM-200CX), X-ray diffractometry (XRD, Rigaku Co. Ltd. RAD-IC system, Cu Kα 40 kV, 20 mA) and electron spectroscopy for chemical analysis (ESCA, ULVAC—PHI ESCA 5600, Al Kα 45°, $3.009712412 \times 10^{-17}$ J (187.85 eV)). However, ESCA results will not be shown in this paper. Complexes of Au and Pt concentrations in the filtrates were estimated by using an inductively coupled plasma atomic emission spectrometer (ICP, Shimadzu Co. Ltd. ICPS-1000 III).

3. Results and discussion

3.1. Selective deposition of gold nanoparticles on well-defined materials

Gold has long been recognized inactive as a catalyst till the advent of the report by Haruta et al., who have demonstrated that gold functions as a highly active catalyst for oxidation of CO to CO_2 when it is deposited as ultrafine particles with high dispersion on metal oxide supports, such as hematite and titania [10,11]. Since the turnover frequency of the CO conversion per unit number of exposed surface Au atoms markedly increased with size reduction, their efforts have been directed towards minimizing the particle size of Au with narrow size distribution [10–16].

As a result, nanometer-sized metallic Au particles were selectively deposited onto monodispersed polycrystalline ellipsoidal hematite particles without addition of any specific reducing agent, as shown in Fig. 1. It seems that Au^{3+} ions of $Au(OH)_nCl_{4-n}^-$ complex, formed by the first aging at room temperature, are reduced to Au particles by electron transfer from the coordinated OH^- ions on the surface of hematite as a catalyst of the electron transfer. As a consequence, the essential reducing agent is water. The optimum pH to yield the maximum quantity of Au particles was ca. pH 5.9, as measured at room temperature, corresponding to the pH of the above standard system. ESCA analysis of Au on the support demonstrates that the resulting solids included mainly metallic Au together with Au oxides.

Au^{3+} ions are reduced to metallic Au^0 by electron transfer from coordinated OH^- ions on the surfaces of hematite particles through their catalytic action. Virtually, ca. 62.5 mol% of Au^{3+} ions was reduced to metallic Au. The analysis of by-products revealed that ClO^-, ClO_3^- and ClO_4^- were produced in the liquid phase in addition to O_2 in the gas phase with stoichiometric concentration. In a separate experiment in which the reduction of Au(III) was performed in the same way but in the absence of chloride ions by using $Au(OH)_3$ gel, almost the same results in yield and particle size of Au were obtained. Hence, chloride ions are unlikely to play a positive role in the reduction of Au(III) in this system. Fig. 2 shows transmission electron micrographs of Au particles supported by (a) monocrystalline ellipsoidal, (B) (b) monocrystalline pseudo-cubic and (c) monocrystalline platelet-type hematite particles (see also Fig. 3 for Au particles on polycrystalline ellipsoidal (A) particles). Fig. 3 shows Au particles deposited on: (a) α-FeOOH, (b) β-FeOOH, (c) ZrO_2 (A), (d) ZrO_2 (B) and (e) TiO_2 (anatase). The yield of AuO(OH) and Au^0 on each support and approximate particle size of the Au^0 are listed in Table 1.

As a rule, the specific surface area is the most important determinant of the yield and size of Au particles for a given kind of support. The larger the specific surface area is, the higher yield and the smaller particle size are obtained, because of the increase in probabilities of reduction and thus of nucleation. The extremely small yield and the large size of Au^0 particles with the platelet hematite are given for this reason. The exceedingly high yields and small sizes with zirconia (A) and

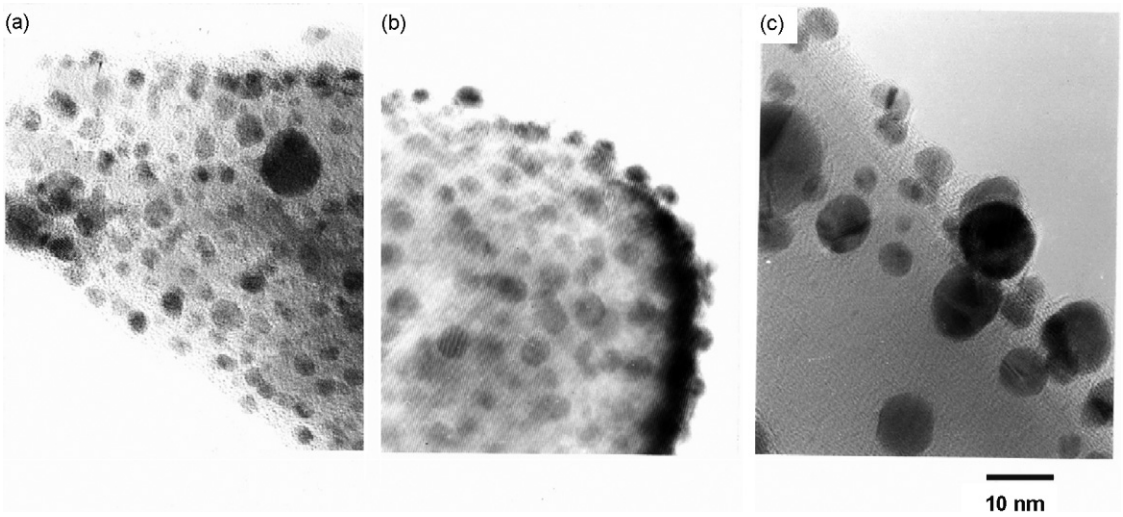

Fig. 2. Au particles deposited on hematite particles different in size and structure: (a) monocrystalline ellipsoid, (b) monocrystalline pseudocube and (c) monocrystalline platelet.

(B) may be explained in a similar manner. The size difference of Au^0 with hematite supports different in specific surface area may also be elucidated based on the same reason. In this case, the yield difference is rather small, because all these systems were close to the saturation of the reaction. However, one may find a significant effect of the species of the support on the yield and final particle size of Au^0. Namely, the yield of Au^0 per unit surface area is particularly high with the ZrO_2 supports and decreases in the order of α-Fe_2O_3, α-FeOOH≃TiO_2, β-FeOOH (the specific surface area of the TiO_2 is estimated to ca. 1.6 times as much as that of monocrystalline ellipsoidal α-Fe_2O_3). Also, the final size of Au^0 per unit surface area is especially small with the ZrO_2 supports and increases in the order of α-Fe_2O_3, TiO_2, α-FeOOH and β-FeOOH. These effects of support species on the yield and size of Au^0 particles are deemed to be elucidated in terms of the catalytic activity of each particle. Nevertheless, in view of the significant difference in the particle size of Au^0 between TiO_2 and α-FeOOH despite

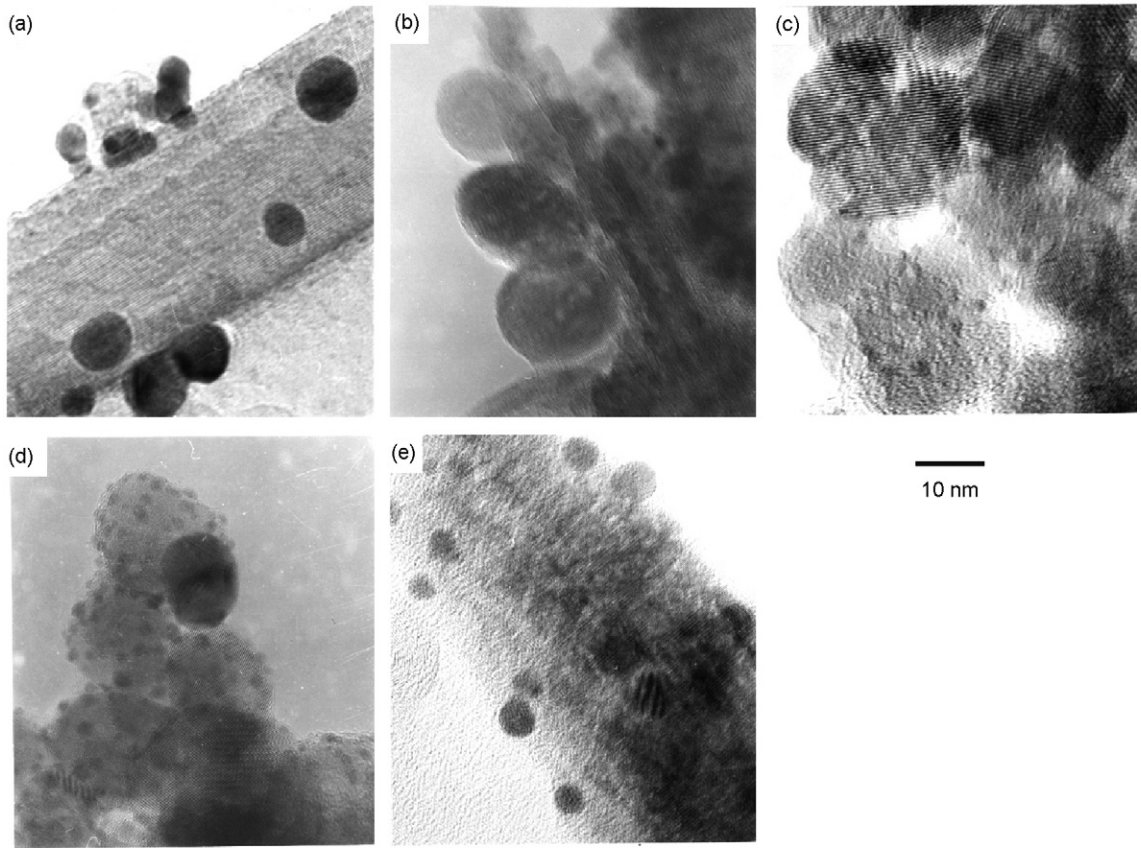

Fig. 3. Au particles deposited on different supports: (a) α-FeOOH, (b) β-FeOOH, (c) ZrO_2 (A) (rough surface), (d) ZrO_2 (B) (smooth surface) and (e) TiO_2 particles.

Table 1
Characteristics of the supports used for deposition of metallic Au particles, yields of the metallic Au and Au hydroxide, and the size of metallic Au particles on the different supports

Supporting particles	Size (μm)	Structure	Specific surface area ($m^2\ g^{-1}$)	Yield (mol%)		Size of Au^0 (nm)
				Au hydroxide	Au^0	
α-Fe_2O_3, ellipsoids (A)	0.20 × 0.038	Polycrystal	136	19.9	75.1	1–2
α-Fe_2O_3, ellipsoids (B)	0.46 × 0.10	Single crystal	21.8	13.8	60.6	2–5
α-Fe_2O_3, pseudocubes	0.09	Single crystal	15.9	10.5	74.7	3–5
α-Fe_2O_3, platelets	13.3 × 1.5	Single crystal	0.70	74.3	8.5	5–15
α-FeOOH, needles	0.50 × 0.020	Single crystal	41.0	18.8	67.6	5–15
β-FeOOH, needles	0.25 × 0.012	Polycrystal[a]	112	10.3	62.7	5–20
ZrO_2 (A), spheres (rough surfaces)	0.015	Single crystal	153	0.6	99.0	0.2–1
ZrO_2 (B), spheres (smooth surfaces)	0.015	Single crystal	118	2.8	95.1	1–3
TiO_2, ellipsoids	0.35 × 0.045	Single crystal		15.8	54.8	2–5

[a] Each needle-like crystal of β-FeOOH is known to consist of a bundle of much thinner subcrystals.

the comparable yields of Au^0, it is likely that the surface roughness also contributes to size reduction of Au^0 by inhibiting the aggregative growth on the support.

Interestingly, we found that gold particles were not produced with monodisperse amorphous SiO_2 particles prepared by the method of Stober et al. [17]. Hence, silica has no catalytic activity for the reduction of Au(III) in the present system.

3.2. Selective deposition of Pt nanoparticles on well-defined materials

Effects of the initial pH on the selective deposition of the precursor particles were investigated. For the Ru, Rh and Pd precipitates, their yields reached 100% at maximum, while the maximum yield of the Ir precipitate was somewhat lower than 100% and that of the Pt precipitate was still lower around 90%. The difference in the maximum yield is due to the difference in solubility of each precipitate, based on the complexation of the metal ions with hydroxide ions. Except for the Ru precipitate, the yield was found to be more or less lowered with decreasing pH in the acidic media, suggesting the precipitates being metal hydroxides or oxides, which are dissolved with decreasing OH^- ions. From the detailed observation by high-resolution transmission micrographs of the as-precipitated nanosized precursor particles on α-Fe_2O_3 ellipsoid support, little pH dependence of the final particle size of each metal compound was found, as compared to the significant metal-species dependence, i.e., ∼0.4 nm for Ru compound, ∼0.7 nm for Rh compound, ∼3 nm for Pd compound, ∼0.6 nm for Ir compound and ∼1.5 nm for Pt compound. In addition, there was no precipitate apart from the support particles for all samples, suggesting that the metal precipitates selectively deposited only on the support particles. This fact implies that the support particles provide specifically stable sites for the deposition of the metal compounds.

As a result of X-ray photoelectron spectroscopy, the as-precipitated metal compounds are mostly characterized by a binding energy higher than that of each bulk metal, suggesting that the precipitates are hydroxides or oxides, in contrast to the case of gold systems in which Au^{3+} ions are mostly reduced to metallic gold on the metal oxide supports. As a consequence, some reduction process is needed for these metal compounds in the platinum group to be reduced to the metallic nanoparticles. Fig. 4 illustrates the yield of the precursor particles changing with aging time, in the presence or absence of the α-Fe_2O_3 ellipsoid support (1.6 g dm^{-3}), showing the precipitation of the precursor kinetically enhanced by the support. These results suggest that the surfaces of the α-Fe_2O_3 ellipsoid support play the role of nucleation centers of the precursor particles. The large precursor particles of 20–50 nm were formed by aging for 72 h in the absence of any support. The size distribution was relatively narrow and each particle consisted of much smaller particles of 2–3 nm. As a consequence, the support plays an important role in the formation of the well-dispersed precursor nanoparticles.

The precursor particles of Pt, $PtO_2{\cdot}nH_2O$, were tried to be deposited on hematite (α-Fe_2O_3) supports: (a) polycrystalline ellipsoid (A), (b) monocrystalline ellipsoid (B), (c) monocrystalline pseudocube and (d) monocrystalline platelet. Also, the precursor particles of Pt were tried to be formed on other supports other than α-Fe_2O_3: (a) α-FeOOH, (b) β-FeOOH, (c) ZrO_2 (A)

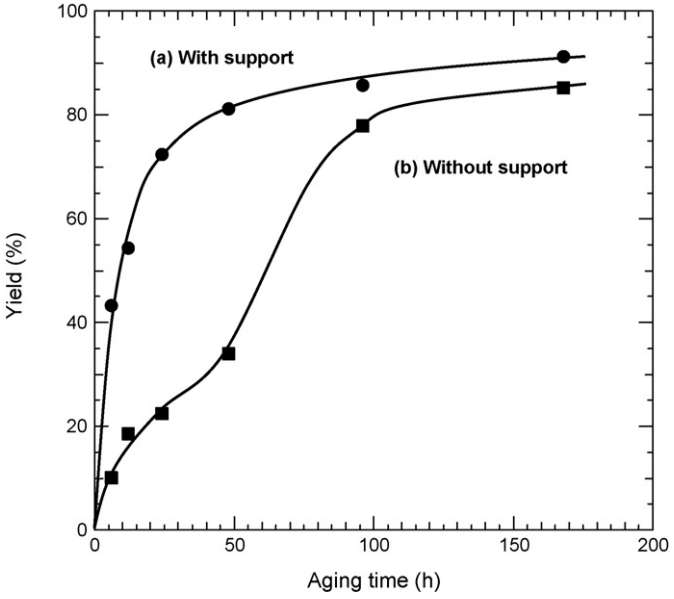

Fig. 4. Changes in the yield of the precursor particles of Pt in the presence (a) and absence (b) of the α-Fe_2O_3 ellipsoid (A) support.

Table 2
Effect of support particle on the size of precursor and metal particles of Pt

Support particles	Specific surface area ($m^2\ g^{-1}$)	Yield (%)	Size of $PtO_2 \cdot nH_2O$ (nm)	Size of Pt (nm)
α-Fe_2O_3, ellipsoid (A)	136	88.8	1.3 ± 0.5	2.0 ± 0.5
α-Fe_2O_3, ellipsoid (B)	12.92	68.5	1.3 ± 0.5	2.5 ± 1.0
α-Fe_2O_3, pseudocube	15.9	50.0	1.5 ± 0.5	2.0 ± 0.5
α-Fe_2O_3, platelet	0.70	46.1	1.5 ± 0.5, 20–30[a]	5.5 ± 2.0[b]
α-FeOOH, needle	41.0	64.0	1.7 ± 0.8, 10–20[a]	–[c]
β-FeOOH, needle	112	75.1	1.3 ± 0.5	–[c]
ZrO_2 (A), sphere (rough surface)	153	84.1	1.5 ± 0.5	2.2 ± 0.5
ZrO_2 (B), sphere (smooth surface)	118	72.4	1.6 ± 0.7	2.4 ± 0.6
TiO_2, ellipsoid (anatase)	37.5	76.2	1.5 ± 0.5	1.3 ± 0.5
None		36.6	20–50	

[a] Size of the particles deposited apart from the support.
[b] Aggregated.
[c] Pt particles could not be observed, since they were occluded into the support drastically deformed by the reduction with H_2 gas.

with rough surfaces, (d) ZrO_2 (B) with smooth surfaces and (e) TiO_2 (anatase), exemplified as Fig. 5. The mean sizes and yield of the precursor particles are summarized in Table 2 with the specific surface area of the supports. For the platelet-type α-Fe_2O_3 and α-FeOOH supports, the large precursor particles independently precipitated apart from the supports, but not for the other supports. As a rule, the specific surface area is the most important determinant of the yield of the precursor particles for a given material of the supports. The larger the specific surface area is, the higher yield is obtained, because of the increase in probability of nucleation. The small yield and some independent precipitation of the precursor particles with the platelet-type hematite support are for this reason. However, the independent precipitation of the precursor particles with the α-FeOOH support may not be explained by the effect of the surface area, since the independent precipitation is not observed with the monocrystalline ellipsoidal α-Fe_2O_3 (B) and TiO_2 supports of rather smaller specific surface areas. This fact may suggest the relatively small affinity of α-FeOOH to the precursor particles. As different from Au particles deposited on various supports, where not only the yield but also the size of Au depended on the surface area, the sizes of the precursor particles of Pt on the different supports were almost the same around 1–2 nm,

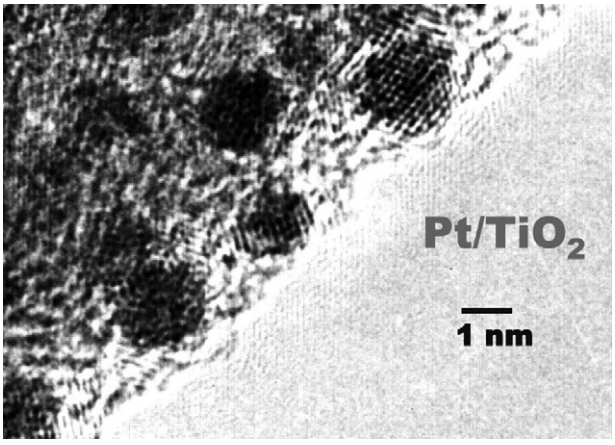

Fig. 5. High-resolution transmission electron micrograph of Pt deposited on spindle type monocrystalline anatase TiO_2 prepared by the selective deposition method.

probably because the mobility of the precursor on the support surfaces necessary for the aggregative growth is extremely small as compared to the metal particles. Incidentally, it seems noteworthy that the internal surfaces of a porous support such as α-Fe_2O_3 ellipsoid (A), measured by the BET method, may not be used for the precipitation of the precursor, since the independent precipitation of the precursor is already observed with 1.2 g dm^{-3} of α-Fe_2O_3 ellipsoid (A) despite its very high specific surface area of 136 $m^2\ g^{-1}$. Hence the distribution of the final Pt particles seems to be limited to the external surfaces of supports. The precursor particles were reduced to Pt particles with H_2 gas at 250 °C for 2 h. For α-FeOOH and β-FeOOH, the original shapes were drastically deformed by the reduction to magnetite and thus the Pt particles occluded into the deformed supports could not be identified. In the case of hematite supports, though it was confirmed by XRD that they were completely converted into magnetite, the original shapes were retained, except for the platelet-type particles partly deformed. The mean size of the Pt particles on the supports but α-FeOOH and β-FeOOH are listed in the last column of Table 2. As a rule, the Pt particles are more or less grown from the precursor particles by coagulation or Ostwald ripening through two-dimensional diffusion of atomic or ionic species of Pt, but one may find a significant effect of the species of the support on the final particle size of metallic Pt. The finest Pt particles were obtained with ellipsoidal TiO_2 (anatase) support, in which the Pt particles appeared rather smaller than the precursor particles, as shown in Fig. 5. In spite of rather random surfaces of TiO_2, only the surface roughness cannot account for this excellent dispersion of Pt. The main reason may be the considerable adsorption amount of Pt precursor complexes from solution phase, since it has been reported that nanometer Ni particles were formed through the preferential adsorption of Ni precursor and the rapid successive nucleation [18]. The detailed formation mechanism will be reported elsewhere.

References

[1] H.C. Yao, M. Seig, H.K. Plummer Jr., J. Catal. 59 (1979) 367.
[2] A. Muramatsu, S. Shitara, H. Sasaki, S. Usui, Shigen-to-Sozai 106 (1990) 799;
A. Muramatsu, H. Sasaki, S. Usui, Sozai Busseigaku Zasshi 5 (1992) 59.

[3] H. Takahashi, S. Myagmarjav, K. Yamamoto, N. Sato, A. Muramatsu, Mater. Trans. 44 (11) (2003) 2414;
S. Myagmarjav, H. Takahashi, Y. Sunagawa, K. Yamamoto, N. Sato, A. Muramatsu, Mater. Trans. 45 (7) (2004) 2035.
[4] H. Arai, Shokubai (Catalyst) 19 (1977) 365.
[5] J.C. Summers, S.A. Ausen, J. Catal. 52 (1978) 447.
[6] B.C. Gates, J.R. Katzer, G.C.A. Schumit, Chemistry of Catalytic Processes, McGraw-Hill, 1979,, p. 184.
[7] P. Wynblatt, N.A. Gjostein, Prog. Solid State Chem. 9 (1975) 21.
[8] M. Boudart, Adv. Catal. 26 (1969) 153.
[9] G.A. Somorjai, Adv. Catal. 26 (1977) 1.
[10] M. Haruta, T. Yamada, T. Kobayashi, S. Iijima, J. Catal. 115 (1989) 301.
[11] M. Haruta, S. Tsubota, H. Kobayashi, M. Genet, B. Delmon, J. Catal. 144 (1993) 175.
[12] S.D. Gardner, G.B. Hoflind, B.T. Upchurch, D.R. Schryer, E.J. Kielin, J. Schryer, J. Catal. 129 (1991) 114.
[13] S.D. Lin, M. Bollinger, M.A. Vannice, Catal. Lett. 17 (1993) 245.
[14] A. Baiker, M. Kilo, M. Maciiejewski, S. Menzi, A. Wokaun, in: L. Guczi, et al. (Eds.), Proceedings of 10th International Congress on Catalysis, Budapest, 1992, Elsevier, Amsterdam, 1993, p. 1257.
[15] S. Tsubota, M. Haruta, T. Kobayashi, A. Ueda, Y. Nakahara, in: G. Poncelet, et al. (Eds.), Studies in Surface Science and Catalysis, vol. 63, Elsevier, Amsterdam, 1991, p. 695.
[16] M. Okamura, K. Tanaka, A. Ueda, M. Haruta, Solid State Ionics 95 (1997) 143.
[17] W. Stober, A. Fink, E. Bohn, J. Colloid Interface Sci. 26 (1968) 62.
[18] H. Takahashi, Y. Sunagawa, S. Myagmarjav, A. Muramatsu, Catal. Survey from Asia 9 (2005) 187.